

Nominal state determination and its effect on remaining useful life prediction

Solichin Mochammad^{1,2} , Nam Ho Kim^{3,*} and Yoojeong Noh^{1,*} 

¹ School of Mechanical Engineering, Pusan National University, Busan, Republic of Korea

² Department of Mechanical Engineering, Sepuluh Nopember Institute of Technology, Surabaya, Indonesia

³ Department of Mechanical and Aerospace Engineering, University of Florida, Gainesville, FL, United States of America

E-mail: nkim@ufl.edu and yooneh@pusan.ac.kr

Received 1 December 2023, revised 28 April 2024

Accepted for publication 20 May 2024

Published 11 June 2024



Abstract

In machinery operation, a prolonged healthy or nominal state often lacks prognostic significance, causing challenges like data overload, biased predictions, and complex models. Moreover, many prediction methods utilize the complete history of monitoring data from the machine's startup to its failure; however, prognostics mostly relies on data from the degradation stage. To address this, this study proposes a method to identify and exclude the prolonged period of the nominal state, thereby enhancing the prediction performance of remaining useful life (RUL). A health index (HI) is formulated by integrating acceleration signals from multiple time windows, with deviations computed as the disparity between the HI and its root mean squares. The identification of start and end times for the nominal state, determined by the intersection of consecutive deviation curves, leads to its exclusion from degradation behaviour modelling. The utilization of polynomial degradation trends from HI data after the nominal state's end time, incorporating a positive slope constraint, aids in mitigating extrapolation uncertainty. The method's efficiency is demonstrated in three defect cases, highlighting improved RUL predictions without the nominal state's inclusion.

Keywords: nominal state, updating features, remaining useful life prediction

1. Introduction

The degradation process in a machine component such as bearings can be represented by a health indicator or health index (HI). The HI encompasses several states prior to actual failures, such as the running-in stage during startup, a nominal state (healthy state), defect initiation, degradation, and damage growth. In real engineering applications, the condition of machines can vary due to differences in load, mechanical systems, and supporting components. HIs play a crucial role in identifying maintenance needs, optimizing performance, ensuring safety, and supporting predictive maintenance, leading to cost savings and extended machine lifetimes. Accurate modelling of these HIs is essential, which involves observing

the degradation process through signal processing from monitoring sensors such as accelerometers [1, 2]. Generally, condition monitoring, through data collection, is essential for predicting remaining useful life (RUL) before equipment or component failures occur [3–6]. This monitoring is part of condition-based maintenance and is considered a prognostic process [7–10], even though some monitoring occurs during all machine states, including the nominal state. However, it is important to note that the entire HI, including the nominal state, may not be effective for prognostics because RUL prediction is primarily influenced by the degradation state.

Including all degradation processes, especially the nominal state can pose several challenges. Firstly, it can lead to high data volume and increased costs due to the extended duration of the nominal state. Secondly, the presence of undamaged states can introduce bias into predictions. Additionally, the substantial difference in trend between the nominal state and

* Authors to whom any correspondence should be addressed.

degradation state makes RUL predictions difficult. Finally, including the nominal state can complicate the functional form of the degradation process. To address these issues and simplify degradation trend modelling, it is necessary to identify and exclude nominal states [11].

Previous research has explored methods for identifying the transition from nominal to degraded states in health monitoring. These methods used the deviation in HIs to predict the degradation point with a threshold [12]. Additionally, the relative rate of change in the mean and variance of HIs were used as a criterion to distinguish the abnormal state from the normal one [13]. Some studies employed supervised learning to predict anomalies in bearings by identifying nominal conditions using historical run-to-failure data [14, 15]. Furthermore, a convolutional autoencoder was utilized to extract input features of degradation and reduce dimensions through a multi-dimensional health state mapping function. When the health status index, calculated using Euclidean distance, falls below a certain threshold, online degradation detection is triggered, and RUL predictions are adaptively updated [16]. Another approach involved clustering degradation data based on operating conditions and using a tailored Transformer model for RUL prediction [17]. It is noteworthy that most of these studies relied on historical run-to-failure data. These studies require future condition data in the training process, while in the case of prognosis training, data are only available up to the current time of operation. This represents a weakness in existing studies where run-to-fail data are used for training while the machine is running without knowing the conditions or data in the future.

In addition to determining the nominal state or the starting time of degradation, predicting the RUL is a crucial step of prognostics [18], given the industry's high demand for accurate and reliable RUL predictions [19–21]. As mentioned earlier, excluding the nominal state can improve RUL prediction accuracy, where the final part of the nominal state serves as the initial degradation time for estimating RUL [22, 23].

Several studies have sequentially predicted the starting time of degradation and RUL. For instance, Ahmad *et al* [24] employed a gradient-based method to identify the degradation starting time and used quadratic regression to estimate the bearing RUL. Li *et al* [25] determined the degradation starting time based on the deviation criterion and applied multi-scale convolutional neural networks (CNN) to enhance RUL prediction. Yang *et al* [26] identified the degradation starting time and predicted RUL using a dual CNN approach. While these studies have demonstrated satisfactory performance, it is important to note that the degradation starting time was determined using run-to-failure monitoring data, without providing a detailed explanation of RUL prediction. Ding *et al* [27] predicted degradation indicators based on compound domain shifts. In addition, they carried out uncertainty predictions using the Bayesian improved probabilistic meta-learning method [28]. Unfortunately, both studies still used run-to-failed data, where in prognostics, the machine or component had failed before it was predicted. Prognostics could

not utilize future monitoring data to identify either the nominal state or degradation initiation.

Removing nominal state data may result in insufficient degradation data for robust RUL prediction, introducing significant uncertainty. To ensure reliable predictions, it is essential to guide the training process toward a monotonic degradation trend [29–32]. By focusing on a monotonically increasing degradation trend, unrealistic RUL predictions can be eliminated, reducing uncertainty. Additionally, RUL prediction should be versatile, and applicable to various failure scenarios, to demonstrate strong predictive capabilities.

Finally, below are summary of challenges in the prognostic process.

1. It is difficult to identify the starting time an anomaly or degradation occurs without referencing to future monitoring data.
2. The prolonged nominal state period can cause a bias in RUL prediction or complicate the prediction model.
3. Due to the small number of data in the degradation stage, it is possible that the degradation model predicts an opposite trend.
4. The level of uncertainty is large in RUL prediction due to a small number of data.
5. It is difficult to generalize the training methodology due to different trend behaviours and nonlinearity.

This study presents a prognostic approach for addressing the above mentioned challenges in predicting the RUL of bearings. This is achieved by determining the nominal state using available information up to the current time and guiding the extrapolation process. The key contributions of the proposed method are as follows:

1. Identification of the starting and ending times of the nominal state by finding the crossing point of consecutive deviation values without relying on future data.
2. By excluding the nominal state from degradation modelling and simplifying RUL prediction into a simple functional form, the model becomes intuitive and easy to use, enabling unbiased RUL predictions with low computational costs.
3. By imposing a monotonicity constraint that accounts for degradation behavior, uncertainty in RUL predictions is reduced.
4. Evaluation of the proposed method in three different bearing failure cases, considering various characteristics like fault mode, run-to-failure time, operating conditions, and loading.

The manuscript is organized as follows: section 2 defines the prognostic problems of predicting RUL with monitoring data, which consists of several degradation phases. Section 3 describes the proposed methods to address the problems. Section 4 introduces the data used to test the proposed method. Section 5 presents the results of the proposed method in determining the nominal state and excluding it from the RUL prediction.

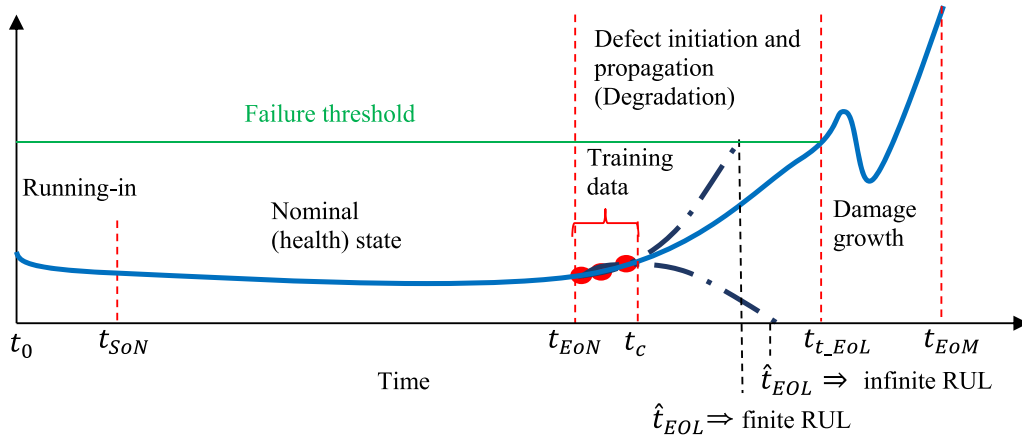


Figure 1. An illustration of the RUL prediction with degradation.

2. Problem definition

Components in rotating machinery, such as bearings, can degrade in performance due to the heavy load imposed on the shaft, leading to wear and damage. Vibration sensors are employed for monitoring anomalies and gathering damage data. Each bearing operates under different conditions including load support, rotation frequency, bearing types, and failure modes, leading to varying degradation trends.

Several studies on bearing performance degradation modelling have presented the variations in degradation processes under different bearing operation conditions [33–35], including (a) slow degradation, (b) accelerated degradation, (c) slow degradation followed by accelerated degradation, and (d) defect initiation and propagation degradation as shown in figure 1. These findings illustrate that:

1. The degradation process is modelled from degradation onset to end-of-life (EoL) due to varying trends in different failure cases, necessitating a universally applicable method.
2. Data from the running-in process and nominal state throughout the entire operating time were excluded from degradation modelling.
3. Figure 1 illustrates the entire degradation process and changes in HI over time, including the operation start time (t_0), nominal state start time (t_{SoN}), the nominal state end time (t_{EoN}), the current time (t_c), the EoL time (t_{EoL}), and monitoring end data (t_{EoM}) under real operating conditions.
4. The nominal state remains stable with little variation for a long time compared to the degradation time, $\sigma_{t_0 \sim t_{EoN}} > \sigma_{t_{EoN} \sim t_{EoL}}$ and $t_0 \sim t_{EoN} > t_{EoN} \sim t_{EoL}$, where σ is the deviation of the degradation trend, as shown in the figure 1.

The condition of degraded bearing is of utmost importance in predicting RUL. The nominal state, unrelated to degradation, should be excluded from prognostic processes to enhance RUL prediction accuracy. Once the nominal state is determined, its end time is used as the initial time of degradation for RUL prediction. The EoL time of the bearing is determined when the degradation value reaches the failure threshold.

Modelling HI at the point where initial degradation occurs after (t_{EoN}) can often lead to false RUL predictions because of insufficient training data. For example, as shown in figure 1, the EoL (\hat{t}_{EoL}) estimated from insufficient degradation data often yields infinite RUL values when the degradation trend decreases. Even if the calculated EoL yields a finite RUL value, significant deviations from the actual EoL value can still produce inaccurate predictions.

3. Proposed method

The proposed method involves two primary stages. In Stage 1, the state of the entire process is determined, encompassing the running-in state, nominal state (excluded for prognostic analysis), degrading state, and damage growth state. Stage 2 involves extrapolating the HI in the degradation state beyond the current time and predicting the RUL.

Stage 1 begins with the data collection, serving as input for the proposed method. The data includes vibration measurements from multiple bearings with varying fault modes and operating conditions. Detailed information about data collection can be found in section 4.

To demonstrate the relationship between amplitude, frequency, and time simultaneously, vibration data is transformed into the frequency domain using FFT and a simultaneous windowing to generate a spectrogram. The highest amplitudes extracted from the spectrogram are then used to obtain the HI values through principal component analysis (PCA). Further details can be found in [36].

As shown in figure 2, Stage 1 aims to determine the starting and end points of the nominal state based on the HI. The HI values from the monitored bearing exhibit various trends, including typical noise found in vibration data signal processing. The HI values are smoothed using the Savitzky–Golay method, which involves a convolution process applying linear least squares to fit subsets with polynomials [37]. Conversely, Stage 2 is dedicated to improving RUL predictions following the identification and exclusion of the nominal state.

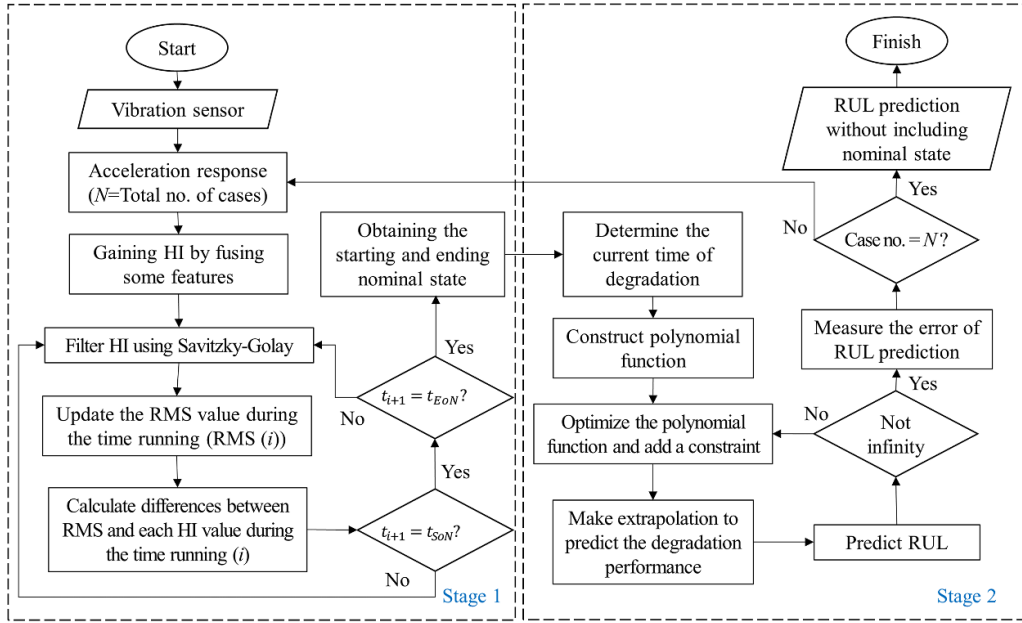


Figure 2. Flowchart of the proposed method.

3.1. Identification of the nominal state

Once the raw HI data are smoothed, they are used to define the history of updated features. Let m be the current time index. Then, the updated features can be defined as

$$F_i^{(m)} = \left| \sqrt{\frac{1}{m} \sum_{k=1}^m Y_k^2 - Y_i} \right| \quad (1)$$

where Y_i is the smoothed HI, and $0 \leq i \leq m$ is the time index. Therefore, $F_i^{(m)}$ represents the updated feature values from the 0 through the m th time index. When a significant HI change occurs at time t_i , the RMS changes gradually because the RMS is affected by all data up to time t_m .

The way to determine the state change is to find a crossing point when the updated feature values at $(m-1)$ and (m) current time intersect in the i th and $(i+1)$ th time indexes. That is, the starting and end points of the nominal state can be identified when the following condition holds:

$$\text{if } F_i^{(m-1)} \langle F_i^{(m)} \text{ and } F_{i+1}^{(m-1)} \rangle F_{i+1}^{(m)}, \text{ then } t_{\text{SoN}} = t_{i+1}. \quad (2)$$

Once the start time of the nominal state is established, the end time can be determined by observing the same condition over an extended period without crossings.

In figure 3(a), the HI trend initially starts high until time index 5. After applying smoothing to the HI data and using equation (1) for updating features with an increment of m , as shown in figure 3(b), the start of the nominal state is pinpointed at time index 4 as it fulfills the conditions in equation (2). Despite several consecutive crossings after time index 4 due to the transition process from an unstable to a stable state (the nominal state), the endpoint of the nominal state is identified when there are no further crossings after time index 6,

signifying the nominal state condition. The end of the nominal state is recognized when the upcoming update time increases until the degradation condition in equation (2) is satisfied.

3.2. RUL prediction

In Stage 2, once the end of the nominal state is identified, degradation prediction is initiated by gradually increasing the number of training data from the end of the nominal state to the current time. The prediction process involves utilizing data to generate a polynomial fit, followed by extrapolation. The degradation model is defined as follows:

$$\hat{Y}(t) = a_0 + a_1 t + a_2 t^2 + a_3 t^3. \quad (3)$$

Where t is the time starting from the end of the nominal state, and a 's are unknown model parameters. In this study, a cubic polynomial is chosen for its ability to effectively capture the nonlinear degradation while maintaining simplicity with a limited number of unknown coefficients. Since degradation typically follows a monotonically increasing pattern, a positive slope is required. Hence, the model parameters are determined by solving a constrained optimization problem that ensures a positive slope:

$$\begin{aligned} \text{Minimize } \text{MSE} &= \frac{1}{N} \sum_{i=t_{\text{EoN}}}^c (Y_i - \hat{Y}_i)^2 \\ \text{Subject to } \frac{d\hat{Y}}{dt} &> 0 \end{aligned} \quad (4)$$

where Y_i represents the i th degradation data, and \hat{Y} is the degradation prediction value from t_{EoN} to t_c with a total of N training data. Note that the mean squared error is calculated using only the training data up to the current time t_c , but the

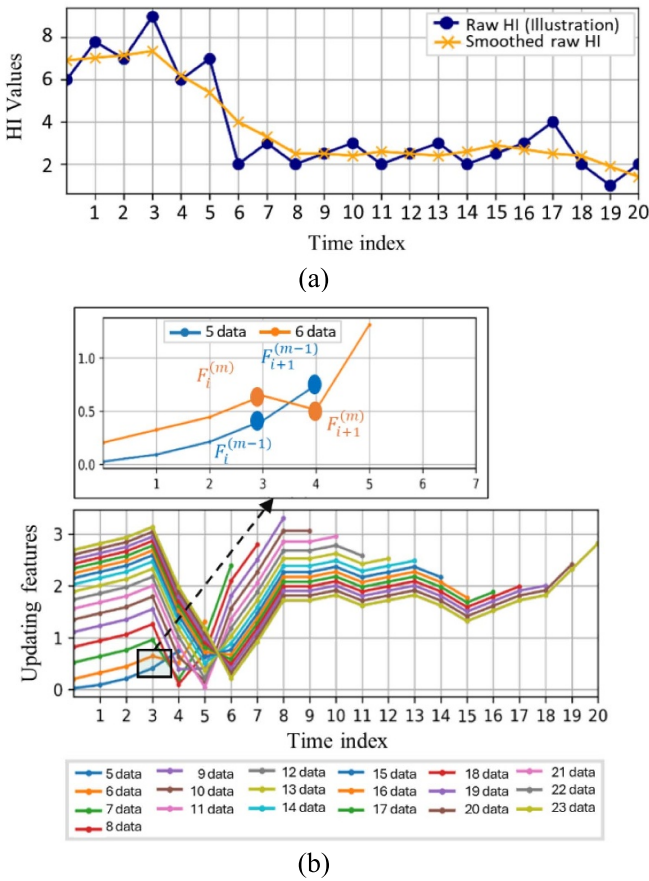


Figure 3. Illustration of the proposed method: (a) synthetic data and (b) identifying the nominal state with updated features.

positive-slope constraint is imposed for all times up to the prediction failure.

The optimization problem is solved using constrained optimization by linear approximation algorithm [36], which employs linear approximation for objective and constraint functions. This optimization is a component of Powell’s conjugate direction method [37].

The RUL is incrementally estimated over time based on predicted degradation values. At the current time t_i , the calculation of the time at which the degradation value exceeds the threshold, $\hat{t}_{\text{fail}}(i)$, is performed using the degradation model. Subsequently, the predicted RUL at t_i is defined as:

$$\text{RUL}(i) = \hat{t}_{\text{fail}}(i) - t_i \quad (5)$$

where \hat{t}_{fail} is the failure time predicted using the proposed method.

4. Data collection

4.1. IMS bearing datasets

The datasets for this study were obtained from experiments conducted by the Center for Intelligent Maintenance Systems (IMS) at the University of Cincinnati [38]. These experiments

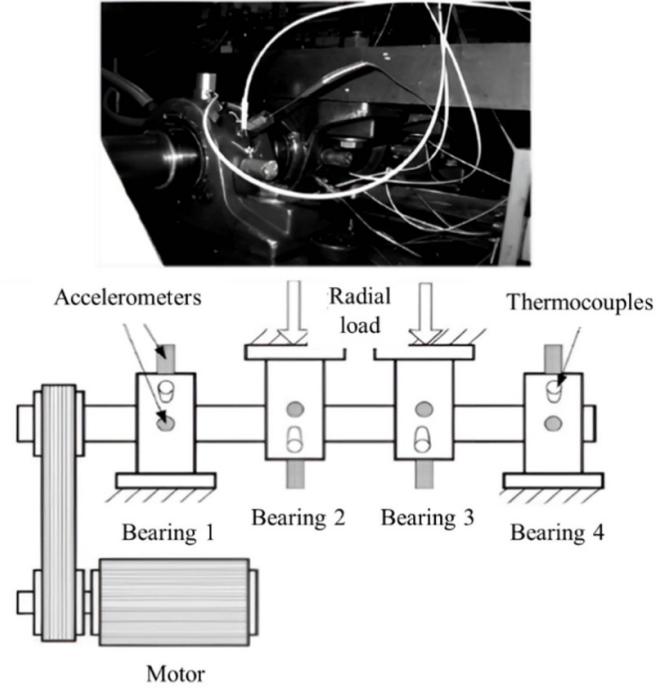


Figure 4. IMS experimental setup [39].

involved multiple bearings on a mechanical system’s shaft, as depicted in figure 4. The experimental setup included a shaft rotating at a constant speed of 2000 rpm, a shaft under a 6000 lbs load, with a Rexnord ZA-2155 bearing, and a high-sensitivity quartz ICP accelerometer (PCB 253B33).

The experiment generated a dataset of bearing vibrations, covering the entire lifespan from a healthy state to failure. Vibration data, captured as acceleration responses, came from bearings with different fault modes. This study specifically focuses on two cases: ‘Case 1’ involving data dimensions of 20480×984 , and ‘Case 2’ with data dimensions of 20480×2156 . The data was intermittently recorded throughout the bearing’s lifespan at a 20 kHz sampling frequency with 20480 sample points. The raw data was then processed to derive HIs using a combination of spectrogram-based features and PCA [36]. The HI is derived from spectral analysis, which involves detecting peak values in all time windows to enhance the model’s accuracy. After completing the extraction from spectral analysis, PCA is used to combine all the extracted data from the time windows, transforming the model dimensions into 2D. Figure 5 illustrates the HIs for both cases.

4.2. PRONOSTIA datasets

Another dataset was obtained from experiments conducted on the PRONOSTIA platform at the FEMTO-ST Institute [40]. Figure 6 illustrates the experimental setup, featuring the bearing and accelerometer sensors used for recording acceleration responses. This experiment aimed to gather vibration monitoring data from the bearing over its entire operational life.

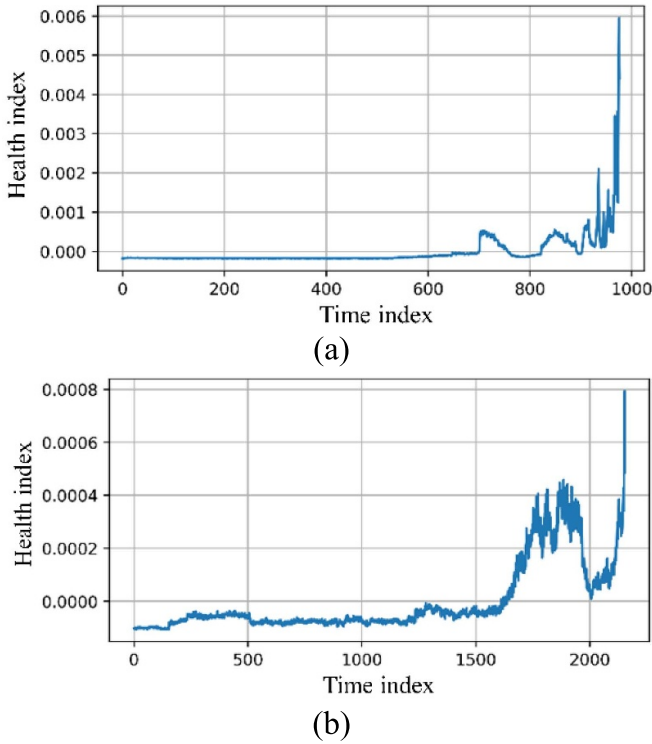


Figure 5. Bearing health index (a) outer race defect and (b) inner race defect.

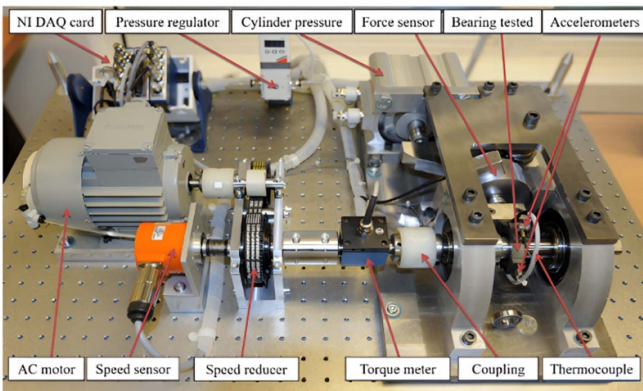


Figure 6. PRONOSTIA experimental setup [41].

To comprehensively understand how various system operating conditions affect bearing degradation, this study incorporates the PRONOSTIA platform data as one of its case studies. In real-world situations, the nature of degradation or failure type is often unknown unless intentionally induced for experimental purposes. However, this study uses a dataset encompassing a range of degradation scenarios resulting from different experimental variables such as rotational speed, load, and operating frequency.

To demonstrate this, the study focuses on one run-to-failure case (Case 3), in which the bearing operates at a speed of 1650 and under a load of 4200 N, exceeding the maximum load capacity of 4000 N to accelerate degradation. The dataset

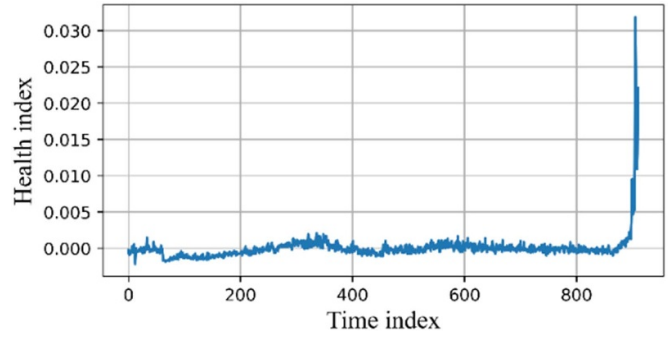


Figure 7. Case 3 (Unknown bearing defect).

dimensions of the dataset for Case 3 are 2559×911 . HI for this case was obtained in the same manner as in the previous study, as depicted in figure 7.

5. Results and discussions

The main goal of this study is to demonstrate the effectiveness of the proposed method in identifying the nominal state and predicting the RUL using the three datasets outlined in section 4. The methodology involves smoothing the HI data and identifying the start and end of the nominal state. Furthermore, the study includes a comparison analysis to assess the performance of degradation and RUL predictions, considering both scenarios: with and without the inclusion of the nominal state.

5.1. Case 1: prognostics of outer-race failure

5.1.1. Nominal state determination for Case 1. The raw HI data contains significant noise, requiring smoothing to reveal the underlying trend. Figure 8 displays both the noisy raw and the clearer smoothed HI trends. The data is truncated at time index 701, as indicated in [34], marking the first time the HI trend crosses the failure threshold through six-sigma analysis. This time index establishes the bearing's EoL.

As seen in figure 8, the smoothed data provides a more evident trend than the raw HI data. These results are employed to determine the initiation and conclusion times of the nominal state. Initially, the HI value starts high as the bearing begins operation and gradually decreases, stabilizing as the bearing reaches a stable state.

Figure 9 illustrates the application of the proposed method to identify the nominal states in Case 1. In figure 9(a), updated features are plotted at interval of 10 data points to reduce computational load. Before the initial crossing, updated features with a higher number of data points exhibit higher values than the previous interval due to lower RMS values, as more HI data becomes available, signifying the bearing's approach to stable operation.

Figure 9(a) indicates the first crossing at time index 59, marking the point of unstable operation until then. Beyond

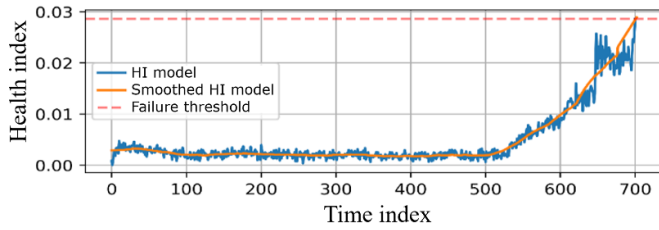


Figure 8. HI from starting operation to EoL in Case 1.

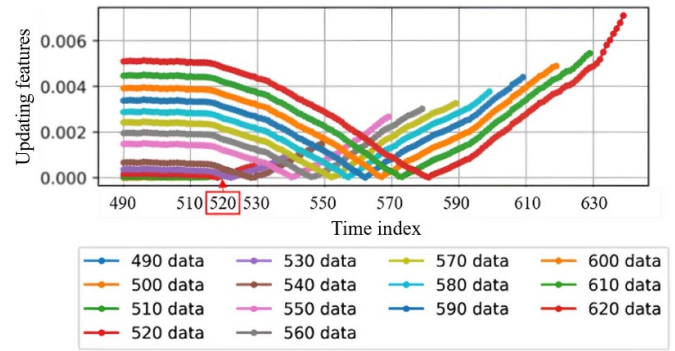


Figure 10. The ending of the nominal state in Case 1.

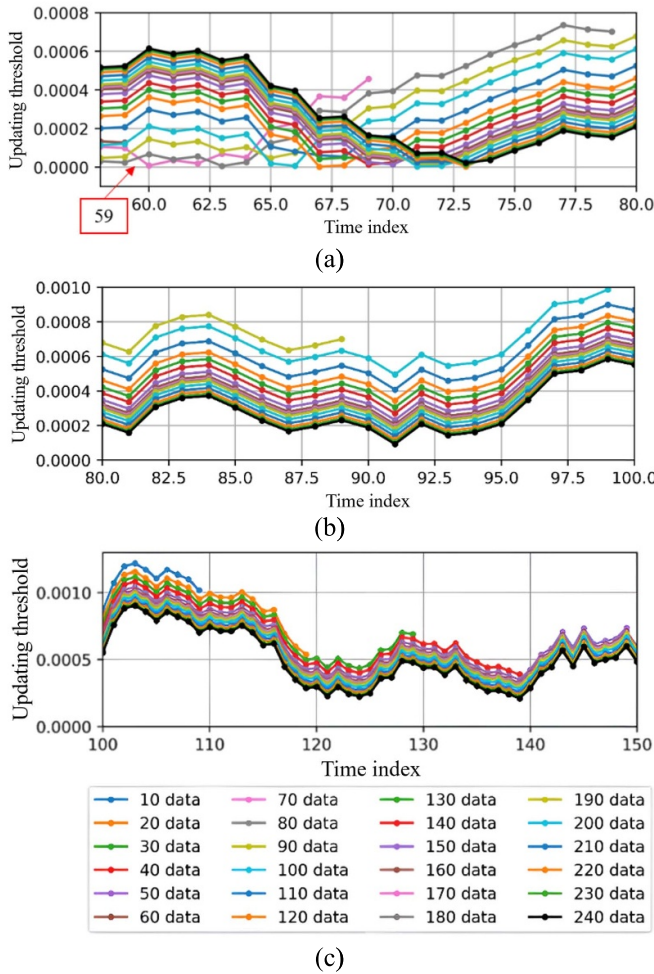


Figure 9. Nominal state start times in Case 1: (a) 52–80 (b) 80–100, and (c) 100–150.

time index 59, additional crossings reflect transitional conditions until the bearing stabilizes into its nominal state. As more data points are added, shown in figures 9(b) and (c), the condition stabilizes with no further crossings after time index 74. This demonstrates the method’s robustness in identifying the initial running-in state and the start of the nominal state.

As mentioned in section 3, a significant increase in HI leads to a crossing between the current and previous time, indicating the onset of bearing degradation. Figure 10 displays this phenomenon, with the crossing at time index 520 in Case 1 marking the end of the nominal state.

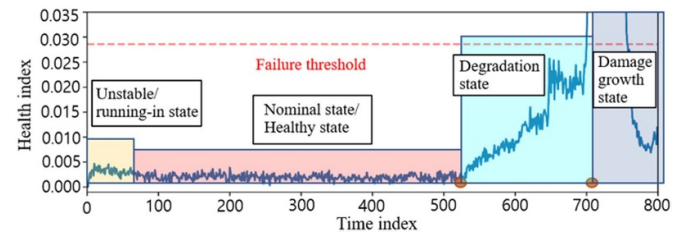


Figure 11. Classification of the degradation phase in Case 1.

In summary, the nominal state in Case 1 commences at the time index 59 and concludes at time index 520, with bearing failure at time index 701. The classification of each state is illustrated in figure 11. The RUL calculation is initiated from the end of the nominal state, simplifying the bearing degradation model by excluding the running-in, nominal state, and damage growth phases.

The results obtained through the proposed method for identifying the nominal state are satisfactory. It is evident that the nominal state exhibits a stable trend, while the unstable, degradation, and damage growth states are marked by non-stationary conditions. This confirms the validity of the proposed method for nominal state determination.

5.1.2. RUL prediction for Case 1. In Case 1, the RUL prediction initiates at time index 520, marking the end of the nominal state. The degradation model is trained incrementally by adding more data to observe its impact on RUL prediction. Figure 12(a) displays RUL predictions using five data points, ranging from time index 520–525. Figure 12(c) illustrates the use of ten training data points, spanning from time index 520–530. Notably, starting with ten data points initially leads to decreasing degradation predictions, which in turn result in an infinite RUL prediction. This issue is resolved by applying a positive slope constraint, resulting in a finite RUL prediction as shown in figure 12(d).

5.1.3. Effect of excluding the nominal state of RUL prediction. Figure 13 compares RUL predictions with and without the nominal state. Excluding the nominal state enhances prediction accuracy, especially with an increasing number of training

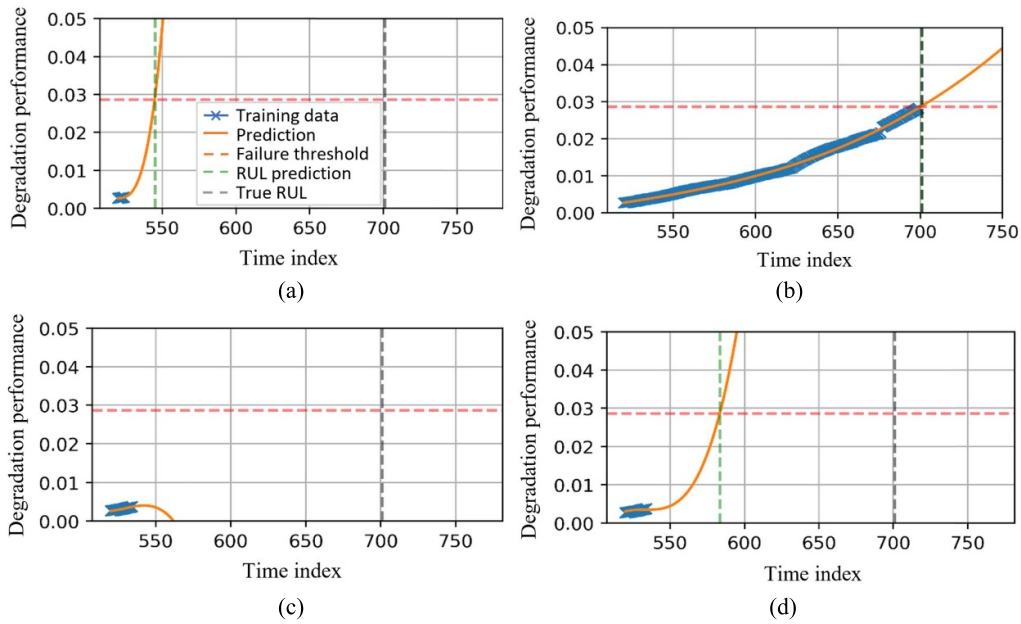


Figure 12. Degradation prediction results in Case 1 using the proposed method, except for (c): (a) 5 training data, (b) 170 training data, (c) 10 training data by extrapolating a cubic polynomial without constraint, and (d) 10 training data.

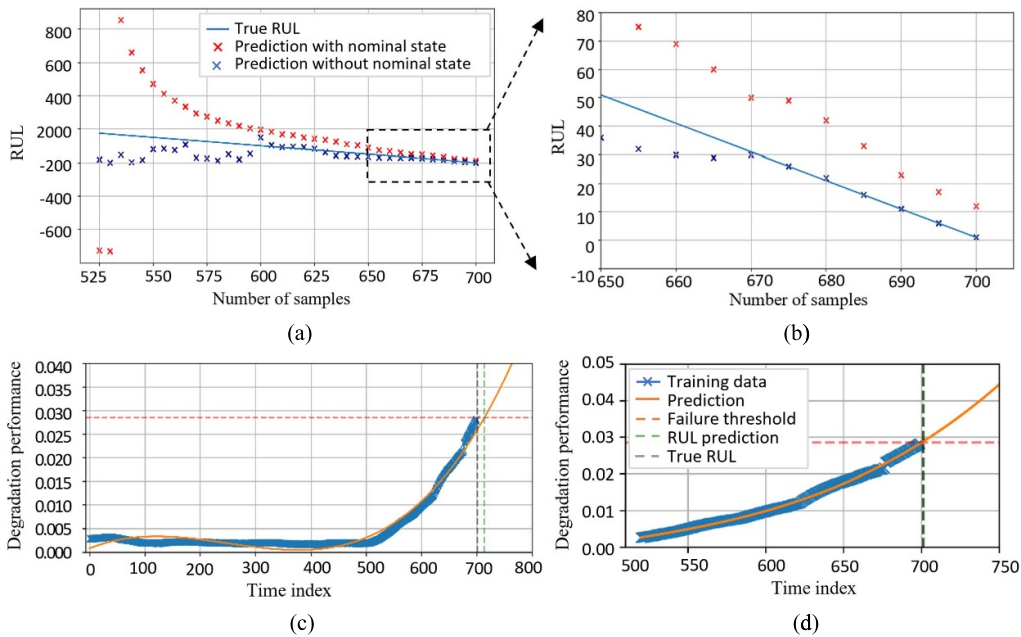


Figure 13. Comparison of RUL prediction with and without the nominal state for Case 1: (a) entire degradation state, (b) detailed view from time index 650–701, (c) including nominal state, and (d) excluding nominal state.

data points, as shown in figures 13(a) and (b). RUL predictions without the nominal state are accurate from time index 650–701, with 701 representing the bearing’s EoL. Furthermore, excluding the nominal state reduces prediction uncertainty and bias.

Figures 13(c) and (d) illustrate that including the nominal state data can lead to biased predictions and violate monotonicity. Accordingly, excluding the nominal state in Case 1 yields satisfactory results. With only five training data points, the model incorrectly predicts the EoL at time index 544

(figure 12(a)), compared to the actual EoL is at 701, indicating substantial prediction errors due to insufficient early samples for extrapolation. Even with ten samples (figure 12(c)), the prediction remains inaccurate. However, applying the positive-slope constraint results in predictions that approach the actual failure threshold, as shown in figure 12(d).

Increasing the number of training data points consistently improves prediction accuracy. With more training data, polynomial extrapolation, guided by the positive-slope constraint, achieves realistic predictions, eliminating unrealistic

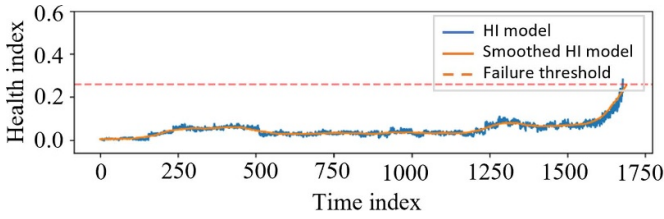


Figure 14. HI from starting operation to EoL in Case 2.

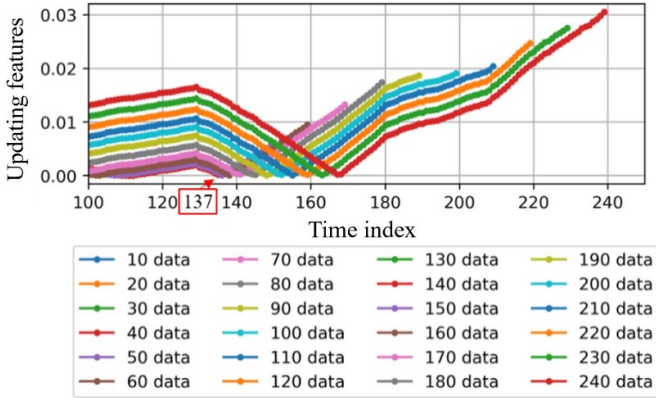


Figure 15. The starting of the nominal state in Case 2.

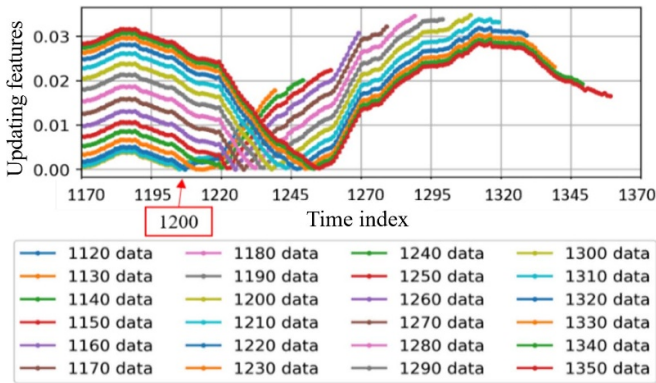


Figure 16. The ending of the nominal state in Case 2.

predictions and ensuring monotonically increasing degradation models, as demonstrated in figures 12(a), (b) and (d).

5.2. Case 2: prognostics of inner-race failure

5.2.1. Nominal state determination for Case 2. In Case 2, the initial trend of HI during operation contrasts with that of Case 1, starting with a low HI value that indicates unstable conditions. Despite this, both cases exhibit noise in the HI data, as depicted in figure 14, which is managed using the same smoothing method. Figures 15 and 16 show the initiation and conclusion of the nominal state in Case 2. The starting point is at time index 137 (figure 15), with crossings continuing until time index 178, indicating a gradual transition. The nominal state concludes at time index 1200 (figure 16), with no further crossings observed up to time index 1260.

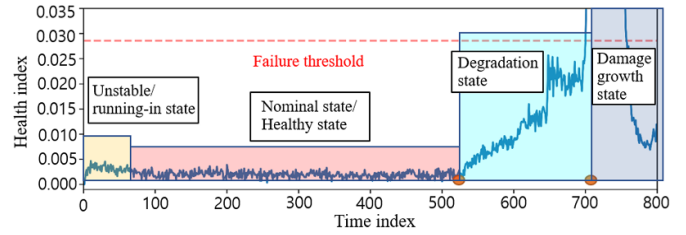


Figure 17. Classification of the degradation phase in Case 2.

To summarize the bearing’s condition, figure 17 provides an overall classification. The monitoring process starts with an unstable running-in condition, followed by the nominal state spanning from time index 137–1200. The degradation state then occurs from time index 1200–1680, during which RUL predictions are made. The final phase corresponds to damage growth in the HI-bearing, commencing at the end of the degradation state and progressing towards EoL.

In figure 17, the overall classification of the bearing conditions is summarized. The bearing monitoring process initiates with an unstable running-in condition, followed by the nominal state spanning from time index 137–1200. Subsequently, the degradation state extends from time index 1200–1680, during which RUL predictions are made. The final stage represents damage growth in the HI-bearing, commencing at the conclusion of the degradation state, ultimately leading to EoL.

5.2.2. RUL prediction for Case 2. During the degradation state, the RUL is estimated by constructing a prediction model for the bearing degradation. This model is developed by training degradation data from time index 1200, gradually increasing the number of training data by 20 until EoL. This dataset presents a challenge as the actual data trend decreases between time index 1300 and 1500.

Figure 18(a) shows the degradation prediction with 20 training data points, where the predicted EoL is still far from the true EoL. This indicates that 20 training data are insufficient for accurately estimating polynomial coefficients. Additionally, several degradation predictions result in unrealistic RUL estimations due to the increasing trend in the extrapolation region, as shown in figure 18(c). However, this decreasing trend can be fixed by imposing the positive slope constraint. Figure 18(d) depicts the change in the prediction trend after applying the proposed method.

5.2.3. Effect of excluding the nominal state of RUL prediction in Case 2. Excluding the nominal state in RUL predictions led to a higher prediction accuracy compared to including the nominal state. When the nominal state was included, the RUL predictions became unconservative, surpassing the actual RUL value after time index 1400. This unconservative poses a problem as it undermines the reliability of maintenance predictions. A similar unconservative pattern emerged when the nominal state was excluded at time index 1570. However, the degree of unconservative prediction was significantly lower, as demonstrated in figure 19.

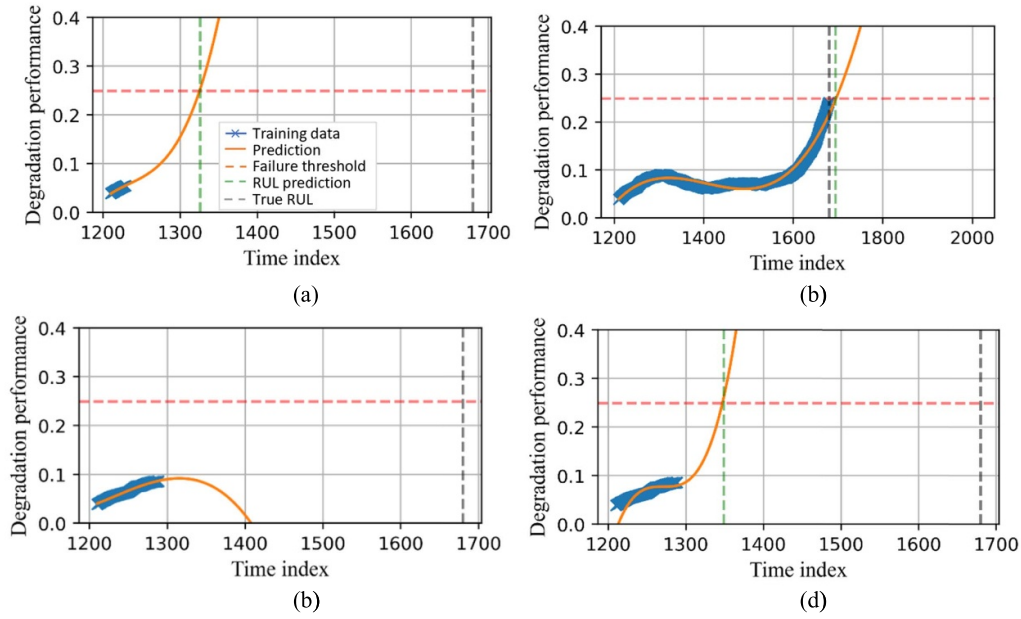


Figure 18. Degradation prediction in Case 2 using the proposed method, except for (c): (a) 20 training data, (b) 470 training data, (c) 80 training data by extrapolating a cubic polynomial without constraint, and (d) 80 training data.

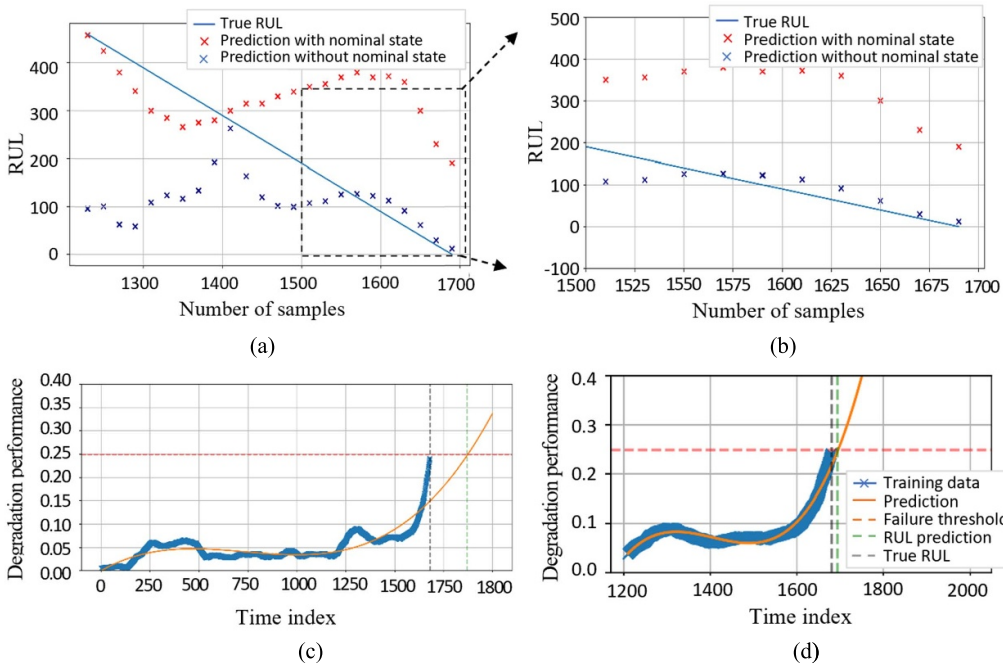


Figure 19. RUL prediction with and without the nominal state in Case 2: (a) RUL prediction on entire degradation state, (b) Zoom-in RUL prediction from time index 1500–1700, (c) RUL prediction including nominal state, and (d) RUL prediction excluding nominal state.

5.3. Case 3: prognostics of unknown failure mode

5.3.1. Nominal state determination for Case 3. The first crossing of updated feature values in Case 3 occurred at time index 47 (figure 20(b)). Subsequent slow transition and fluctuating trends led to additional crossings up to time index 520. Beyond this point, no further crossings were detected until the failure state was reached. Consequently, the transition period was considered part of the nominal state. Figure 21 illustrates

the crossing of feature values at time index 870, occurring after the state had stabilized with no further crossings, indicating the end of the nominal state. The updated feature values then increased rapidly post-time index 870. Figure 21 displays these changes, categorized into two distinct trend groups, either below or within the green dashed-line box, indicating whether the number of data points is less than or greater than 910, respectively.

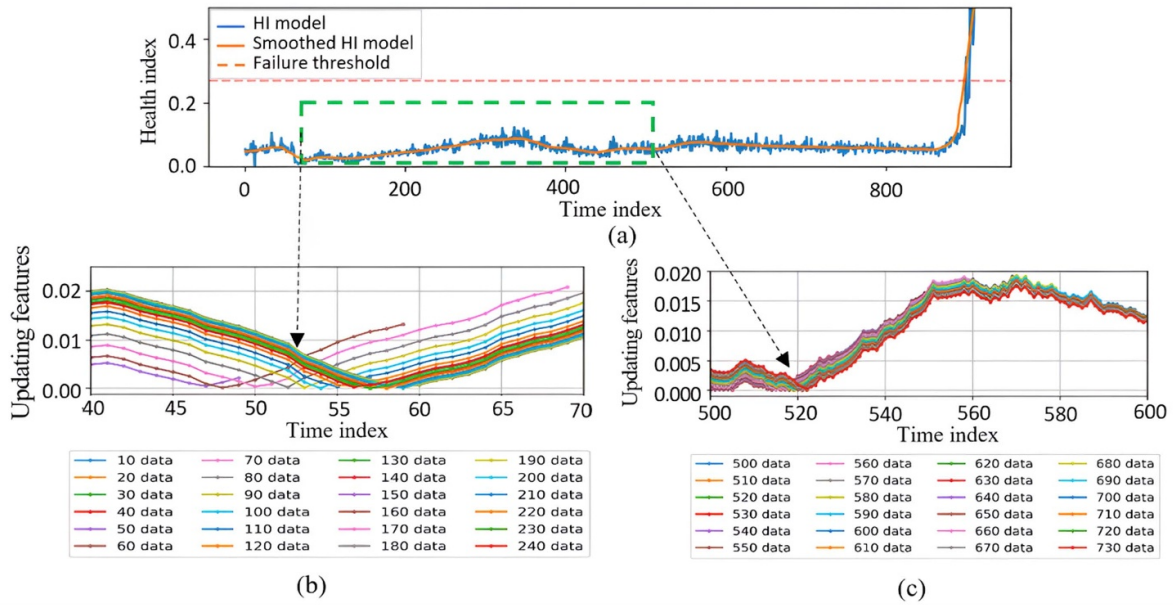


Figure 20. Determination of nominal state in Case 3: (a) HI from starting operation to EoL, (b) starting of the nominal state in Case 3, and (c) ending of the transition from unstable to nominal state.

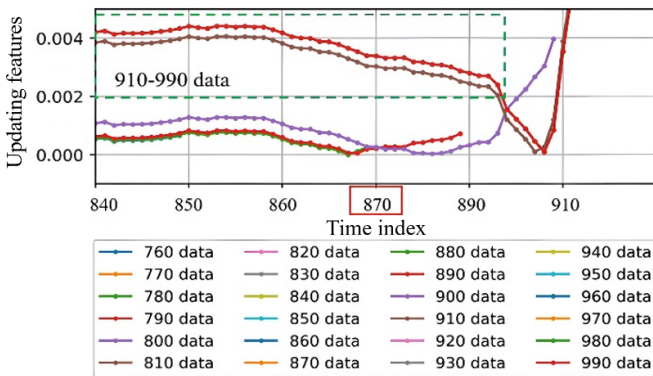


Figure 21. The ending of the nominal state in Case 3.

Notably, a significant deviation is observed in the upper group, with updated features having 910–990 data points. This deviation primarily stems from the utilization of data points within the 910–990 range, resulting in a notably higher degradation value compared to the value observed before the time index of 910. The proposed feature updating method heavily depends on data deviation to update degradation values.

Figure 22 indicates that the significant degradation deviation in Case 3 is due to a sudden failure, occurring without prior degradation initiation after passing through the nominal state. Consequently, using data beyond 910 according to our method results in a drastic increase in feature value compared to using fewer than 910 data points.

In Case 3, the HI states are summarized in figure 22 as follows:

- Time indices 0-56: Running-in state.
- Time indices 56–870: Nominal state.

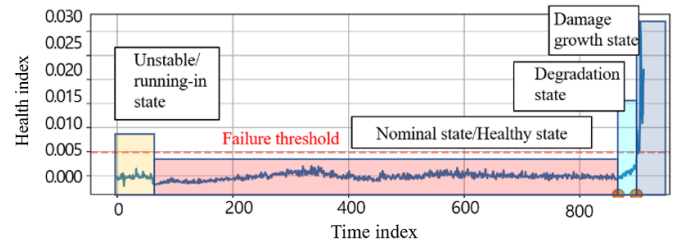


Figure 22. Classification of the degradation phase in Case 3.

- Time indices 870–900: Degradation state (used for RUL prediction).
- Time index 900: EoL in Case 3.
- Time indices 900–911: Damage growth in the bearing.

5.3.2. RUL prediction for Case 3. Case 3 experiences rapid degradation from a healthy state to failure, resulting in limited degradation data. To address this limitation, degradation predictions in Case 3 are trained with an additional five data points. Figure 23(a) illustrates early degradation predictions using only these five data points, from time indices 870–875, as training data. However, this small number of training data points proves inadequate for accurate RUL predictions.

Degradation prediction performance in Case 3 significantly improves when the amount of training data is increased up to the EoL, as shown in figure 23(b). This approach closely matches the actual degradation model and yields better RUL estimates. In contrast, using incorrect degradation models results in unrealistic RUL predictions, as seen in Cases 1 and 2, demonstrated in figure 23(c). Utilizing the proposed third order polynomial extrapolation with positive slope constraints,

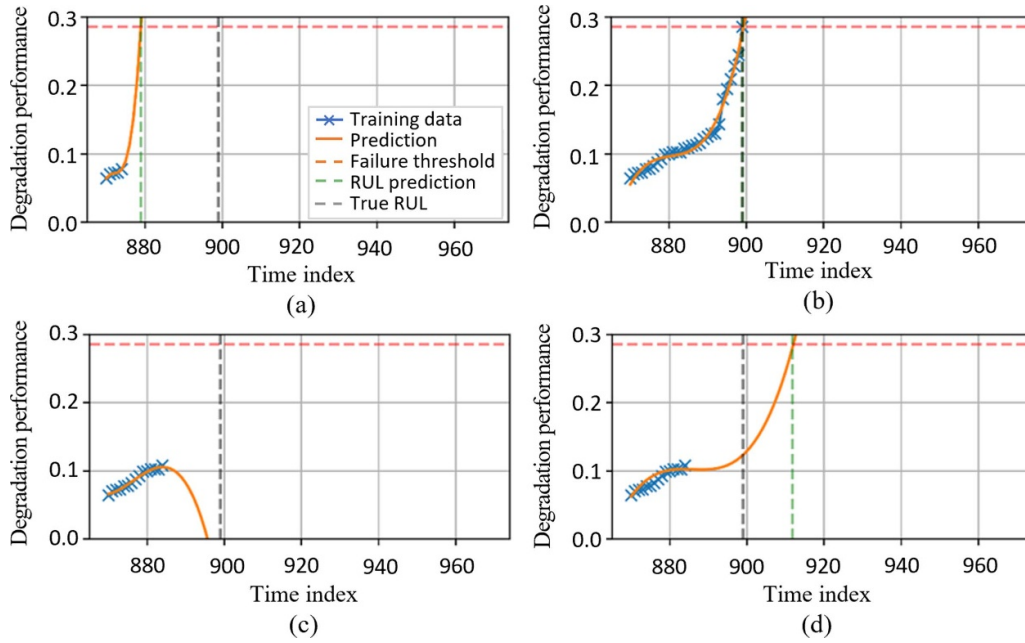


Figure 23. Degradation prediction in Case 3 by applying the proposed method except (c): (a) 5 training data, (b) 20 training data, (c) 15 training data by extrapolating a cubic polynomial, and (d) 15 training data.

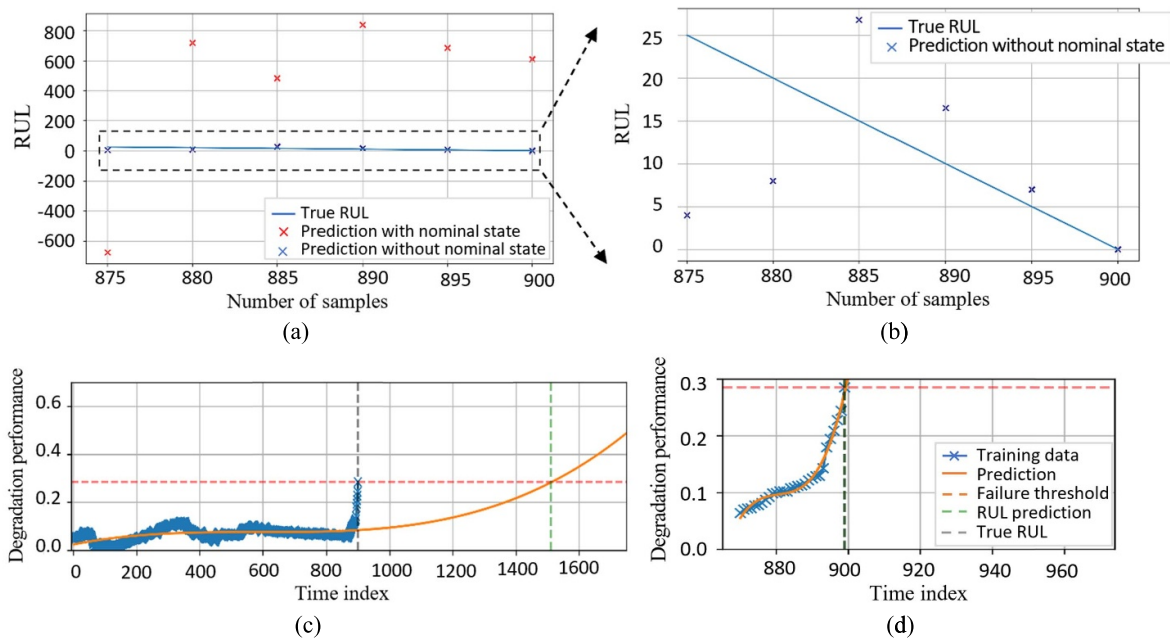


Figure 24. Comparison of RUL prediction with and without the nominal state in Case 3: (a) RUL prediction on entire degradation state, (b) Zoom-in RUL prediction from time index 875–900, (c) Including nominal state, and (d) Excluding nominal state.

as shown in figure 23(d), provides a more realistic prediction of bearing degradation.

5.3.3. Effect of excluding the nominal state of RUL prediction in Case 3. RUL predictions that exclude the nominal state demonstrate improved accuracy compared to those that include it, as illustrated in figure 24(a). Figure 24(b) provides

an enlarged view of RUL predictions without the nominal state, showing how closely these predictions approach the true RUL. On the contrary, RUL predictions that incorporate the nominal state deviate significantly from the true RUL, as shown in figures 24(c) and (d). These figures provide an example of fitting degradation to predict RUL at time index 900, both excluding and including the nominal state, respectively. The exclusion of the nominal state results in a curve that

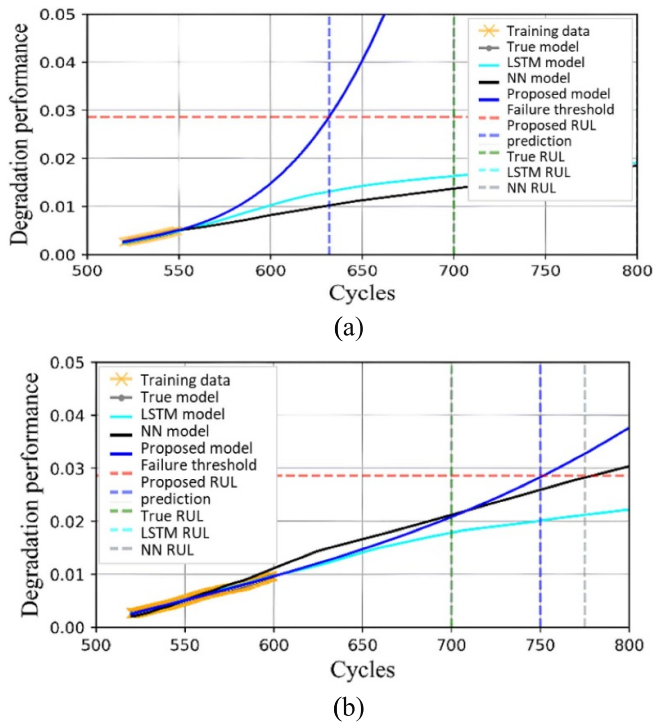


Figure 25. Comparison of method performances: (a) Training data until the current time at cycles 550, and (b) Training data until the current time at cycles 600.

fails to follow the data trend due to the substantial influence of a larger number of data points in the nominal state. Meanwhile, including the nominal state results in a curve that accurately fits the data trend, leading to an accurate prediction of the EoL.

5.4. Comparison of the proposed RUL prediction and other methods

The performance of the proposed method was compared with two other popular approaches for predicting time series data, neural networks (NN) and long-short-term memory (LSTM), using the Case 1 datasets. Figures 25(a) and (b) show the degradation models derived using each method with data up to the 550th cycle (30 data points) and 600th cycles (80 data points), respectively.

As the figure illustrates, while LSTM and NN show high predictive accuracy within the range of the training data, their performance significantly drops in predicting future conditions where no data is available, resulting in RUL estimates that extend to infinity. As the amount of training data increases to 600 cycles, the predictions from LSTM and NN improve since they are closer to the actual EoL, compared to using data limited to 550 cycles. On the other hand, the proposed method, by employing a simplified monotonic increasing polynomial function, can estimate the EoL relatively accurately, especially at the onset of initial degradation, thus enabling high RUL predictions.

6. Conclusions

This study introduces a novel method for determining the nominal state using updated HI data without relying on future data. The method calculates the deviation of HI for each new data point and computes the difference between consecutive HI values. The crossing points in these deviations serve as indicators for the start and end of the nominal state. By excluding the nominal state, the degradation model is simplified, leading to improved accuracy in RUL predictions.

Furthermore, the study presents a technique for predicting degradation performance and RUL. This approach employs third-order polynomial extrapolation with constraints that ensure a realistic degradation model by enforcing a positive gradient.

The proposed method's generality and effectiveness were assessed across three distinct bearing failure cases, each with varying operating conditions and degradation behaviours. The results demonstrated successful identification of the nominal state using updated HI data in all three cases. Additionally, applying constraints to the degradation prediction led to monotonic models and realistic RUL estimations. Notably, RUL predictions excluding the nominal states exhibited higher accuracy, reduced uncertainty, and lower bias compared to those that included the nominal state.

It is important to note that this study is entirely data-driven and does not incorporate machine learning or physical modelling approaches. Future research may explore the potential benefits of combining these methods to leverage machine learning's capacity to predict complex functions and physical model's ability to provide more representative degradation performance predictions, ultimately achieving a more accurate and robust RUL estimation. On the other hand, to prove the visibility and increase the credibility of the proposed method, it will be implemented using measurement data from machines in real industrial problems.

Data availability statement

The data that support the findings of this study are openly available at the following URL/DOI: https://doi.org/10.1007/978-94-015-8330-5_4 and www.damtp.cam.ac.uk/user/na/NA_papers/NA2007_03.pdf.

Acknowledgments

This work was supported by the National Research Foundation of Korea (NRF) grant funded by the Korea government (MIST) (No. 2020R1A5A8018822, 2021R1A2C1013557 and 2022H1D3A2A01052491

ORCID iDs

Solichin Mochammad  <https://orcid.org/0000-0002-4294-788X>

Yoojeong Noh  <https://orcid.org/0000-0003-0342-5189>

References

- [1] Cui L, Wang X, Wang H and Ma J 2020 Research on remaining useful life prediction of rolling element bearings based on time-varying Kalman filter *IEEE Trans. Instrum. Meas.* **69** 2858–67
- [2] Tran V T, Pham H T, Yang B-S and Nguyen T T 2012 Machine performance degradation assessment and remaining useful life prediction using proportional hazard model and support vector machine *Mech. Syst. Sig. Proc.* **32** 320–30
- [3] Zhao Z, Bin L, Wang X and Lu W 2017 Remaining useful life prediction of aircraft engine based on degradation pattern learning *Reliab. Eng. Syst. Saf.* **164** 74–83
- [4] Jardine A K S, Lin D and Banjevic D 2006 A review on machinery diagnostics and prognostics implementing condition-based maintenance *Mech. Syst. Signal Process* **20** 1483–510
- [5] Haidong S, Junsheng C, Hongkai J, Yu Y and Zhantao W 2019 Enhanced deep gated recurrent unit and complex wavelet packet energy moment entropy for early fault prognosis of bearing *Knowl.-Based Syst.* **188** 105022
- [6] Baptista M, Henriques E M P, de Medeiros I P, Malere J P, Nascimento C L and Prendinger H 2019 Remaining useful life estimation in aeronautics: combining data-driven and kalman filtering *Reliab. Eng. Syst. Saf.* **184** 228–39
- [7] Luo Z, Wang J, Tang R and Wang D 2019 Research on vibration performance of the nonlinear combined support-flexible rotor system *Nonlinear Dynam.* **98** 113–28
- [8] Deutsch J and He D 2018 Using deep learning-based approach to predict remaining useful life of rotating components *IEEE Trans. Syst. Man Cybern. Syst.* **48** 11–20
- [9] Jin X, Sun Y, Que Z, Wang Y and Chow T W S 2016 Anomaly detection and fault prognosis for bearings *IEEE Trans. Instrum. Meas.* **65** 2046–54
- [10] Elforjani M and Shanbr S 2018 Prognosis of bearing acoustic emission signals using supervised machine learning *IEEE Trans. Ind. Electron.* **65** 5864–71
- [11] Duong B P, Khan S A, Shon D, Im K, Park J, Lim D-S, Jang B and Kim J-M 2018 A reliable health indicator for fault prognosis of bearings *Sensors* **18** 3740
- [12] Li X, Zhang W, Ma H, Luo Z and Li X 2020 Data alignments in machinery remaining useful life prediction using deep adversarial neural networks *Know-Based Syst.* **197** 105843
- [13] Xu L, Pennacchi P and Chatterton S 2020 A new method for the estimation of bearing health state and remaining useful life based on the moving average cross-correlation of power spectral density *Mech. Syst. Signal Process* **139** 106617
- [14] Zhu W, Ni G, Cao Y and Wang H 2021 Research on a rolling bearing health monitoring algorithm oriented to industrial big data *Measurement* **185** 110044
- [15] Wu B, Li W and Qiu M 2017 Remaining useful life prediction of bearing with vibration signals based on a novel indicator *Shock Vib.* **2017** 8927937
- [16] Xu W, Jiang Q, Shen Y, Xu F and Zhu Q 2022 RUL prediction for rolling bearings based on convolutional autoencoder and status degradation model *Appl. Soft Comput.* **130** 109686
- [17] Xu D, Xiao X, Liu J and Sui S 2023 Spatio-temporal degradation modeling and remaining useful life prediction under multiple operating conditions based on attention mechanism and deep learning *Reliab. Eng. Syst. Saf.* **229** 108886
- [18] Lei Y, Li N, Guo L, Li N, Yan T and Lin J 2018 Machinery health prognostics: a systematic review from data acquisition to RUL prediction *Mech. Syst. Signal Process* **104** 799–834
- [19] Lee J, Wu F, Zhao W, Ghaffari M, Lia L and Siegel D 2014 Siegel D. Prognostics and health management design for rotary machinery systems—reviews, methodology and applications *Mech. Syst. Signal Process* **42** 314–34
- [20] Ali J B, Chebel-Morello B, Saidi L, Malinowski S and Fnaiech F 2015 Accurate bearing remaining useful life prediction based on Weibull distribution and artificial neural network *Mech. Syst. Signal Process.* **56–57** 150–72
- [21] Li N, Lei Y, Lin J and Ding S X 2015 An improved exponential model for predicting remaining useful life of rolling element bearings *IEEE Trans. Ind. Electron.* **62** 7762–73
- [22] Ahmad W, Khan S, Islam M and Kim J 2019 A reliable technique for remaining useful life estimation of rolling element bearings using dynamic regression models *Reliab. Eng. Syst. Saf.* **184** 67–76
- [23] Wang B, Lei Y, Li N and Li N 2020 A hybrid prognostics approach for estimating remaining useful life of rolling element bearings *IEEE Trans Reliab.* **69** 401–12
- [24] Ahmad W, Khan S and Kim J 2018 A hybrid prognostics technique for rolling element bearings using adaptive predictive models *IEEE Trans. Ind. Electron.* **65** 1577–84
- [25] Li X, Zhang W and Ding Q 2019 Deep learning-based remaining useful life estimation of bearings using multi-scale feature extraction *Reliab. Eng. Syst. Saf.* **182** 208–18
- [26] Yang B, Liu R and Zio E 2019 Remaining useful life prediction based on a double-convolutional neural network architecture *IEEE Trans. Ind. Electron.* **66** 9521–30
- [27] Ding P, Zhao X, Shao H and Jia M 2023 Machinery cross domain degradation prognostics considering compound domain shifts *Reliab. Eng. Syst. Saf.* **239** 109490
- [28] Ding P, Jia M, Ding Y, Cao Y, Zhuang J and Zhao X 2024 Machinery probabilistic few-shot prognostics considering prediction uncertainty *IEEE ASME Trans. Mechatronics* **29** 106–18
- [29] Javed K, Gouriveau R, Zerhouni N and Nectoux P 2015 Enabling health monitoring approach based on vibration data for accurate prognostics *IEEE Trans. Ind. Electron.* **62** 647–56
- [30] Liu K, Gebrael N Z and Shi J A 2013 Data-level fusion model for developing composite health indices for degradation modeling and prognostic analysis *IEEE Trans. Autom. Sci. Eng.* **10** 652–64
- [31] Tse P W and Wang D 2017 Enhancing the abilities in assessing slurry pumps' performance degradation and estimating their remaining useful lives by using captured vibration signals *J. Vib. Control.* **23** 1925–37
- [32] Liao L 2014 Discovering prognostic features using genetic programming in remaining useful life prediction *IEEE Trans. Ind. Electron.* **61** 2464–72
- [33] Liu S and Fan L 2022 An adaptive prediction approach for rolling bearing remaining useful life based on multistage model with three-source variability *Reliab. Eng. Syst. Saf.* **218** 108182
- [34] Lim C K R and Mba D 2015 Switching Kalman filter for failure prognostic *Mech. Syst. Signal Process* **52–53** 426–35
- [35] El-Thalji I and Jantunen E 2015 Dynamic modelling of wear evolution in rolling bearings *Tribol. Int.* **84** 90–99
- [36] Mochammad S et al 2022 Fault deterioration modelling of bearings combined with spectrograms and PCA 2022 *KSME Conf. (Jeju, South Korea)*
- [37] Liu J, Li T, Tang Q, Wang Y, Su Y, Gou J, Zhang Q, Du X, Yuan C and Li B 2022 The life prediction of PEMFC based on group method of data handling with Savitzky–Golay smoothing *Energy Rep.* **8** 565–73

- [38] Lee J, Qiu H, Yu G and Lin J (Rexnord Technical Services) 2007 IMS, University of Cincinnati. "Bearing data set" *NASA Prognostics Data Repository* (NASA Ames Research Center) (available at: www.nasa.gov/content/prognostics-center-of-excellence-data-set-repository) (Accessed 10 January 2023)
- [39] Powell M J D 1994 A direct search optimization method that models the objective and constraint functions by linear interpolation *Advances in Optimization and Numerical Analysis* ed S Gomez and J-P Hennart (Kluwer Academic) p 51–67
- [40] Nectoux P, Gouriveau R, Medjaher K, Ramasso E, Morello B, Zerhouni N and Varnier C 2012 PRONOSTIA: an experimental platform for bearings accelerated life test *Int. Conf. on Prognostics and Health Management (Denver, CO, USA, 10 January 2023)* Institute of Electrical and Electronics Engineers (IEEE) www.nasa.gov/content/prognostics-center-of-excellence-data-set-repository
- [41] Powell M J D 2007 A view of algorithms for optimization without derivatives *Cambridge University Technical Report DAMTP 2007/NA03*